Predicting aerosol size distribution development in absorption columns

Hammad Majeed[a] Magne Hillestad[a] Hanna Knuutila[a] Hallvard F. Svendsen[a]*

[a]*Norwegian University of Science and Technology, Trondheim 7491, Norway*

First Author:
Hammad Majeed

Norwegian University of Science and Technology

E-mail address: hammad.majeed@ntnu.no

Second Author:

Magne Hillestad

Norwegian University of Science and Technology

E-mail address: magne.hillestad@ntnu.no

Third Author:

Hanna Knuutila

Norwegian University of Science and Technology

E-mail address: hanna.knuutila@ntnu.no

Fourth and Corresponding Author:

*Hallvard F. Svendsen

Norwegian University of Science and Technology

E-mail address: hallvard.svendsen@ntnu.no

Corresponding author. Tel.: +47-95141784

Predicting aerosol size distribution development in absorption columns

Hammad Majeed[a] Magne Hillestad[a] Hanna Knuutila[a] Hallvard F. Svendsen[a]*

[a]*Norwegian University of Science and Technology, Trondheim 7491, Norway*

Abstract:

There are two main mechanisms for amine emissions from absorption columns. The first is connected to the volatility of amine, determining the gaseous concentration. The second mechanism is via aerosol droplets containing amine. Recently, aerosol based emissions in g/Nm^3 were identified from typical PCCC plants (Khakharia et al., 2013). Mechanisms for aerosol formation, aerosol growth, emissions related to aerosol formation and in particular the development and testing of aerosol emission reducing systems for amine based post-combustion, are presently under study. However, there is still limited information available in the open literature.
In some recent studies, the effect of water wash and demisting equipment was studied and results indicate that aerosol droplets still pass through these equipment sections. On the other hand, water wash systems help in increasing the droplet size as well as reducing both gas phase and aerosol based emission. However, this does not completely solve the problem (da Silva et al., 2013). Recently, modeling studies for mono-disperse droplet swarms are published (Majeed et al., 2017b, 2017a; Majeed and Svendsen, 2018a, 2018b). However, results for multi-sized droplet swarms and for droplet size distributions are missing.

Droplets can be described by their size, temperature and composition. All droplet populations will have a size distribution, being just as important as any other parameter. Performing a distribution analysis is the best way to determine the sizes of droplets in a particular stream at any point in an absorber.

In this work, both a multi-droplet size model and a size distribution model are implemented. The multi-droplet size model is used for validation and results are in line with findings from the mono-disperse model by (Majeed et al., 2017b; Majeed and Svendsen, 2018a). Droplet distribution model results are compared with experimental data from Toshiba (Fujita, 2017) and reasonable agreement is found. The development of inlet droplet distributions through an absorber and water-wash system is modelled for several flue gas sources. It is found that the outlet distribution mean size increases with inlet gas CO_2 concentration. Similarly, the outlet mean droplet size decreases and the size distribution width increases with incoming droplet number concentration.

Keywords: Post combustion CO_2 capture, Absorption columns, Aerosol formation, Amine emissions, Multi droplet model, Droplet size distribution, Orthogonal collocation method, Simulation

Introduction:

Meeting world energy requirements and at the same time control greenhouse gas emissions, is a vital challenge of the current era. It is generally accepted that man-made CO_2 emissions to the atmosphere are a main contributor to the global climate change. Combustion and industrial use of fossil fuels are main sources of CO_2 emissions as society is asking for more and more energy to fulfill its demands (Dutcher et al., 2015).

In order to enable sustainable use of these sources and meet energy requirements, carbon capture via amine scrubbing is an advanced and robust option. 30 wt.% aqueous Monoethanolamine (MEA) solution is often considered as a base case solvent for post combustion carbon capture plants (Abu-Zahra, 2009; Rochelle, 2009).

Formation of aerosols in industrial exhaust gas purification processes can cause serious complications. Small aerosol droplets formed in these processes cannot be removed in conventional demisting equipment and lead to high amine emissions in the exhaust gases. This is today maybe the main obstacle to success and widespread implementation of large scale post combustion capture technology for climate protection (Moser et al., 2015; Schaber, 1995).
In order to understand the mechanisms behind aerosol formation in absorption columns, several experimental investigations have been performed based on injecting foreign nuclei.
Mitsubishi Heavy Industries, Ltd. (MHI) performed pilot pant testing and reported that amine emissions increase in the presence of SO_3 in the flue gas (Kamijo et al., 2013). (Khakharia et al., 2013) studied the effect of soot particles on emissions and stated that with an increase in number concentration of soot particles, MEA emissions also increased.
(da Silva et al., 2013) reported emissions studies from a carbon capture plant at Maasvlakte coal power plant in Rotterdam. They introduced a demister unit for the removal of very fine mist particles of less than 2 microns and the results indicate that the demisting unit was relatively efficient in reducing amine emissions.
Koch-Glitsch has designed mist eliminators for different industrial purposes and report that droplets larger than 10 microns are completely removed. However, as the droplet size decreases below 10 micron, the efficiency of the demisting equipment decreases and the efficiency drops to 40% percent for 5 micron droplets (Koch, 2015). It is reported in experimental and modelling investigations (Khakharia et al., 2013; Majeed et al., 2017a) that aerosol droplets containing amines can be, at least initially, of sub-micron sizes, so demisting units are thought to be less effective.
In order to understand how aerosol droplets grow in absorber columns, a rigorous model is required that can explain how the particle characteristics change in terms of internal composition as well as droplet growth or shrinkage. For this purpose, a model was developed and used to explain how various inlet droplets shrink or grow through an absorption column and water wash section and how their composition is changing with respect to time. (Majeed et al., 2017b, 2017a; Majeed and Svendsen, 2018a, 2018b). These articles describe the model equations for the gas and aerosol phase which are coupled with reaction, equilibrium and heat and mass transfer models along with example cases showing how different parameters like initial droplet size and composition, droplet number concentration and operating parameters of PCCC plants influence the final outlet droplets. These articles deal only with mono-disperse droplet swarms. In the present work, we expanded the model to handle droplet size distributions, which of course is the reality and a most important factor when characterizing aerosol droplets in typical PCCC plant.
Generally, the interest and importance of understanding droplet size dynamics in the industry has increased considerably over the last decade. Many spray applications such as fire suppression and spray drying rely on this information for effective spray use. In the paint industry narrow droplet size distributions are required, while some need wide ones. Other spray processes require very few small drops as in agricultural or consumer products. A class based distribution histogram can give a good overall picture to understand the properties of the product (Ashgriz, 2011), but a size distribution model is, in our view, more appropriate.

Droplet Size Distribution Model:

In order to model a droplet size distribution, the rate of growth of every aerosol droplet size should be known. The model presented in (Majeed et al., 2017a) describes the growth of a droplet as the rate of change in volume with respect to time.

$$\frac{dV}{dt} = \frac{N_{total} \cdot A}{\rho_{droplet}} = \widetilde{N} \cdot A \tag{1}$$

Where N_{total} is the total mass flux of transferring components, e.g. amine, CO_2 and water. V, A and $\rho_{droplet}$ represent the varying droplet volume, surface area and density and $\widetilde{N}$ is the volumetric flux into the droplet. This droplet model is the basis for how the distribution will change with respect to time. It is also assumed that the droplets will not break or coalesce. Breakage of sub-micron droplets is extremely energy demanding, and very high energy density is needed, see (Luo and Svendsen, 1996; Marchetti and Svendsen, 2012). Coalescence is also unlikely, as the particles mainly follow the gas. However, when the particles become very small, i.e. around 10 nm, Brownian motion may occur which may lead to collisions and coalescence. This effect is not included in the model.

When droplets become of a size similar to the mean free path for the molecules of the gas phase, i.e. the Knudsen number becomes close to one, the mass and heat transfer to and from the droplets is reduced significantly. This is taken into account in the model through a reduction factor in the mass transfer coefficient which is a function of the Knudsen number as given by (Fuch and Sutugin(1970) and Davies (1982)). This becomes important when the inlet droplets are small and mainly consist of water. Water will evaporate quickly and droplets can become very small, e.g. 10-20 nm. The Kelvin effect, increasing the vapor pressure over small droplets, is also taken into account. The effect of convective mass transfer is also accounted for and becomes significant when high evaporation or condensation rates for water affect the MEA mass transfer.

In previous articles, only monodisperse droplet swarms have been treated. In reality the aerosols have a droplet size distribution both upon entering the absorber and when they exit the wash section and enter a demisting device. Size distributions can be modelled in different ways. The most direct way is to split the distribution into size classes. In order to represent a distribution well, a relatively large number of classes should be used. This would lead to a heavy numerical load and long execution times. In the current work, we have chosen to represent the size distribution by two droplet sizes, one representing the mean of the distribution and the other representing a measure of the width.

With a large population of droplets, the population distribution function f can be characterized by a continuous function in the volume V. The population distribution function f will change with time and is, therefore, a function f (t,V). We require that the integral of the population distribution over all sizes is unity at any time.

$$\int_0^\infty f(t,V)dV = 1 \tag{2}$$

The population distribution may be approximated by two parameters, the number average volume $\overline{V_1}$ and size average volume $\overline{V_2}$, and the population distribution can be approximated by these two moments as (Ashgriz, 2011; Biesenberger and Sebastian, 1983):

$$\overline{V_1} = \int_0^\infty V f(t,V) dV = \langle V \rangle \tag{3}$$

$$\overline{V_2} = \frac{\int_0^\infty V^2 f(t,V) dV}{\int_0^\infty V f(t,V) dV} = \frac{\langle V^2 \rangle}{\langle V \rangle} \tag{4}$$

The ratio between these two parameters, $\overline{V_1}$ and $\overline{V_2}$, describes the width of the distribution. The larger the ratio, the wider the distribution.

The change in volume average with respect to time is equal to the time derivative of the number average volume:

$$\frac{d\overline{V_1}}{dt} = \langle \frac{dV}{dt} \rangle \quad = \langle \widetilde{N}_1 A \rangle = \widetilde{N}_1 \langle A \rangle \tag{5}$$

It is here assumed that the mass flux into all $\overline{V_1}$ droplets is the same.

The time derivative of the size average volume, i.e. how it is changing with respect to time, can be written as;

$$\frac{1}{\overline{V_2}} \frac{d\overline{V_2}}{dt} \quad = \frac{1}{\langle V^2 \rangle} \frac{d\langle V^2 \rangle}{dt} - \frac{1}{\overline{V_1}} \frac{d\overline{V_1}}{dt} \tag{6}$$

The time derivative of the average square volume is;

$$\frac{d\langle V^2 \rangle}{dt} \quad = 2 \langle V \frac{dV}{dt} \rangle \quad = 2 \langle V A \widetilde{N}_2 \rangle \tag{7}$$

Now, by inserting Eq.5 and 7 in Eq. 6, the final derivative of the size average volume with respect to time will take the form;

$$\frac{d\overline{V_2}}{dt} \quad = \frac{2}{\overline{V_1}} \langle V \widetilde{N}_2 A \rangle - \frac{\overline{V_2}}{\overline{V_1}} \widetilde{N}_1 \langle A \rangle \quad = \frac{2}{\overline{V_1}} \widetilde{N}_2 \langle V A \rangle - \frac{\overline{V_2}}{\overline{V_1}} \widetilde{N}_1 \langle A \rangle \tag{8}$$

$$A = V^{2/3} \frac{4\pi}{\left(\frac{4\pi}{3}\right)^{2/3}} \tag{9}$$

Then $\langle A \rangle$ will be;

$$\langle A \rangle = \frac{4\pi}{\left(\frac{4\pi}{3}\right)^{2/3}} \int_0^\infty V^{2/3} f(t,V) dV \tag{10}$$

Similarly $\langle VA \rangle$ will be ;

$$\langle VA \rangle = \frac{4\pi}{\left(\frac{4\pi}{3}\right)^{2/3}} \int_0^\infty V^{5/3} f(t,V) dV \tag{11}$$

In order to calculate the average $\langle VA \rangle$ and average $\langle A \rangle$, we need to assume a probability density function f. Since V > 0, a log normal distribution is often used to approximate the size distribution of aerosols as (Johnson et al., 1994);

$$f(V) = \frac{1}{V\sigma\sqrt{2\pi}} exp\left(-\frac{(\ln V - \mu)^2}{2\sigma^2}\right) \tag{12}$$

Where V is the volume limit over which the function is integrated, σ is the variance and μ indicates the mean.

The variance and mean can be defined as;

$$\sigma = \sqrt{ln \frac{\overline{V_2}}{\overline{V_1}}}$$

$$\mu = ln\, \overline{V_1} - \frac{1}{2}\, ln \frac{\overline{V_2}}{\overline{V_1}}$$

The calculated average $\langle VA \rangle$ and average $\langle A \rangle$ are than used in equations 5 and 8 for the average change in volume with respect to time.

Result and discussions:

In order to perform modelling of droplet size distributions, a discrete aerosol droplet model is required. For that purpose modelling work performed in (Majeed et al., 2017b, 2017a; Majeed and Svendsen, 2018b) is used as a basis for the current work. Column specifications and liquid phase profiles are described in these articles. These articles describe the basis for the model development in Matlab and how the composition and growth profiles are generated throughout the column and in the water wash sections. These papers also present results on the effect of initial droplet size, droplet number concentration and composition of droplets on the final size and on amine emissions. These topics are thus not discussed here.

One limitation in previous models is that they only deal with one droplet size with specific initial conditions and number concentration. In the current work, a multi droplet model is introduced, so an inlet droplet distribution can be implemented and the initial composition and size can be varied. Still, however, the inlet droplet swarm, having a size distribution, is assumed to have a uniform chemical composition and temperature.

As a first step, in order to simplify and reduce the computational time, and also for model validation, a two droplet size model is introduced. In this model, two droplet swarms, with different droplet sizes (diameters), and in principle different initial composition and number concentration, are fed to the absorber and water washes in the inlet gas stream. For absorber and water wash details see (Majeed et al., 2017b, 2017a; Majeed and Svendsen, 2018b). These validation cases are defined as Case 1a-c as described in Table 1. Further, a droplet inlet size distribution is defined and the model validated against data from Toshiba in Case 2 (Fujita, 2017). Finally the size distribution model is used to investigate how inlet gas CO_2 content and droplet number concentration affect the outlet size distribution.

Table 1: Modelled cases

Case 1a	Two droplets, having same initial sizes of 0.3µ, containing 5M MEA travelling from bottom to top of column (0-19 m)
Case 1b	Two droplets, having same initial sizes of 0.3µ, with different initial compositions: 1st drop: 0.0001M MEA, 2nd drop: 5M MEA (0-19 m)
Case 1c	Two different initial size droplets, containing 0.0001M MEA travelling from bottom to top of column 1st drop: 0.3µ, 2nd drop: 0.6µ (0-19 m)
Case 2	Droplet size distribution from PCC Pilot Plant in Mikawa Power Plant of Toshiba corporation (Fujita, 2017). Validation against experimental data.
Case 3	Droplet distribution on different flue gases: Two different initial size droplets, containing 0.0001M MEA travelling from bottom to top of column 1st drop: 0.3µ, 2nd drop: 0.34µ (0-19 m)

Model verification, Case 1:

In the first validation test we use two droplets having the same initial composition and diameters i.e. 5M MEA and 0.3µ, which travel with the gas phase through the absorber and water wash sections. Submicron size aerosol droplets, as reported in experimental investigations, e.g. in (Khakharia et al., 2013; Moser et al., 2015) are used. Most of the modelled results presented in (Majeed et al., 2017a; Majeed and Svendsen, 2018b) deal with this droplet size range.

The growth profiles are presented in Figure 1a, indicating the validity of the model as both the droplet profiles follow each other. The results are in agreement with the work presented for the single droplet model (Majeed and Svendsen, 2018b).

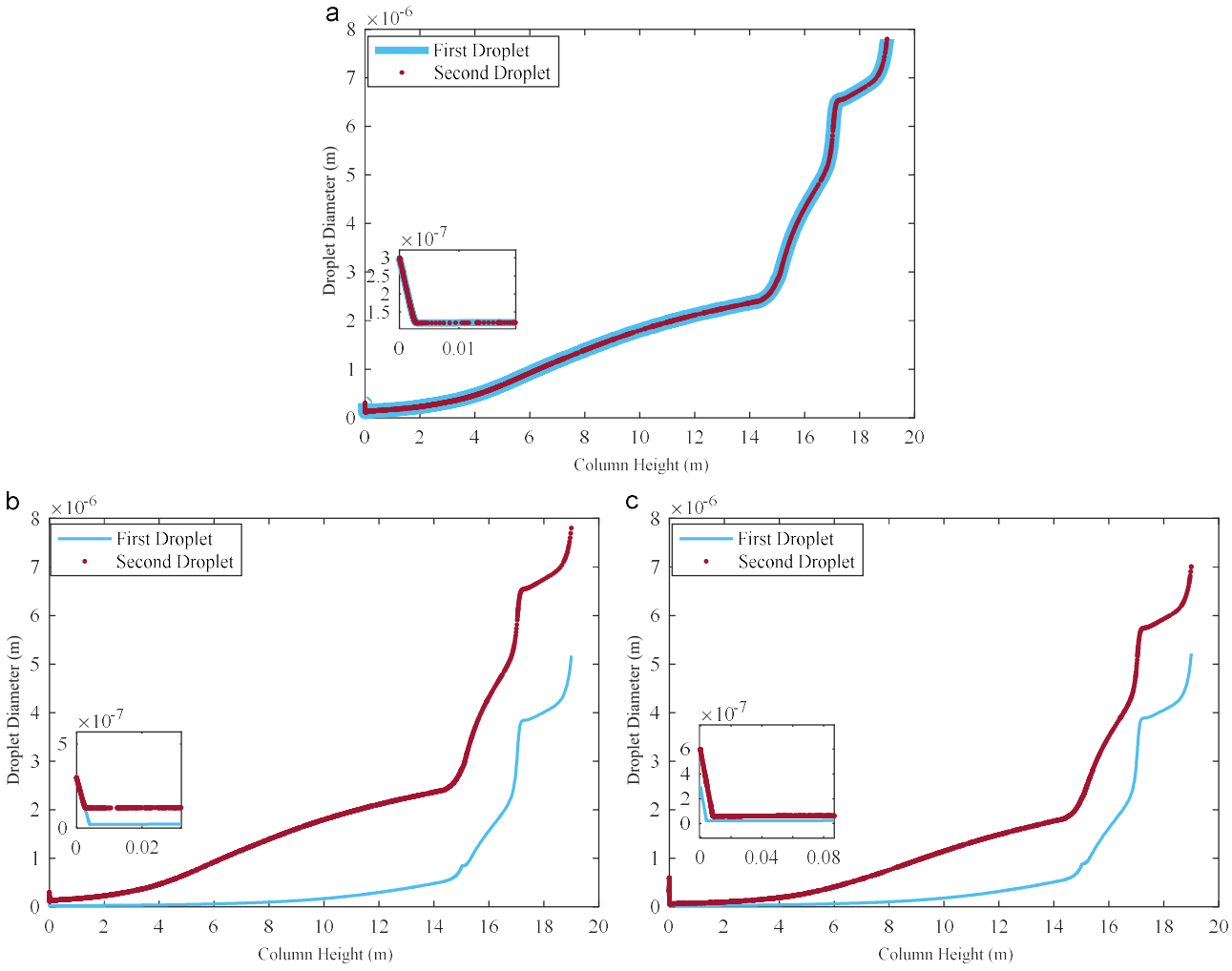

Figure 1: (a) Droplet Growth, Case 1a (b) Droplet Growth, Case 1b, (c) Droplet Growth, Case 1c

In a second test, the initial composition of one droplet is changed to see the effect on growth profiles and to validate the model. The first droplet has an initial diameter of 0.3µ and enters together with the gas phase containing pure water. The second droplet enters with the same initial size, 0.3µ, but with the composition of 5M MEA. The growth profiles are presented in Figure 1b. The results are in agreement with results from the single droplet model for the two specific droplets, see (Majeed and Svendsen, 2018b).

In a third test, the initial size of one droplet is changed while the composition is kept constant. The droplets have different initial diameters of 0.3μ and 0.6μ respectively, but the same composition of pure water. The growth profiles are presented in Figure 1c and are in agreement with results from the single droplet model.

In conclusion, the validation study shows the multi-droplet model to be consistent with the previously developed single droplet model.

Case 2:

At a coal fired power plant in Mikawa, Toshiba has constructed a 10 ton-CO_2/day pilot scale plant. They tested the Toshiba solvent (TS-1) and also compared the results with conventional 30 wt% MEA. Amine emissions and mitigation techniques were main focal points in their recent campaigns and results indicate that water wash systems are less effective in reducing these emissions than anticipated.

In order to further validate our droplet size distribution model we have selected and modelled two of the Toshiba cases in which they give both the inlet and outlet aerosol size distributions for coal based flue gas with 30 wt% MEA, The absorption column has 5 packing sections of 3 meter each. The capture rate was 90% and the flue gas flow rate was 2100Nm^3/hr. (Fujita, 2017; Fujita et al., 2017). The liquid phase profiles are presented in figure 2. We may have slight difference in water washes as Toshiba worked with single water wash with height of around 3- 4m meters, whereas we have two water washes of 2m each. Toshiba have not provided any further column characteristics.

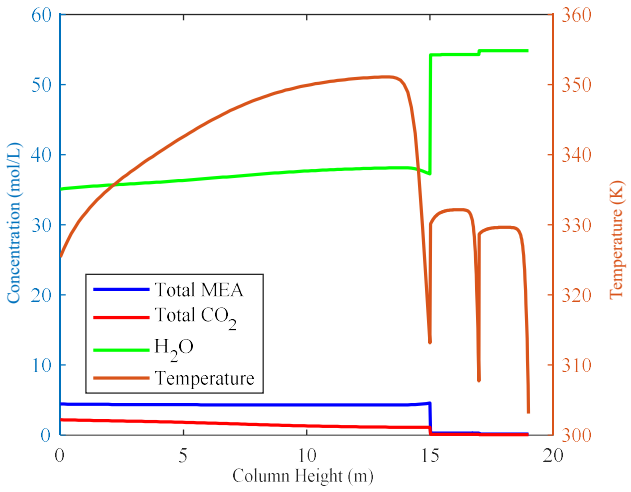

Figure 2: Liquid phase profiles for Case 2

According to (Fujita, 2017), at the absorber inlet, the droplet diameters range from 10-440 nanometres (nm). They have also indicated the droplet swarm peak size and number concentration. The choice of peak size and droplet number concentration from the results they have provided is somewhat uncertain, as these two parameters vary a lot depending on operational point in time. In the first validation test, we have selected a peak size of 60 nm.

The inlet droplet number concentration is given as around 200000 drops/cm^3. In the model studies, we have chosen number concentrations ranging from c_N = 1-6.10^5 drops/cm^3, in order to cover a wider range.

The droplet inlet size distribution we have used, and which is assumed to represent the first Toshiba case with a peak size of 60nm and with sizes ranging from 10-440 nm, is presented in Figure 2.

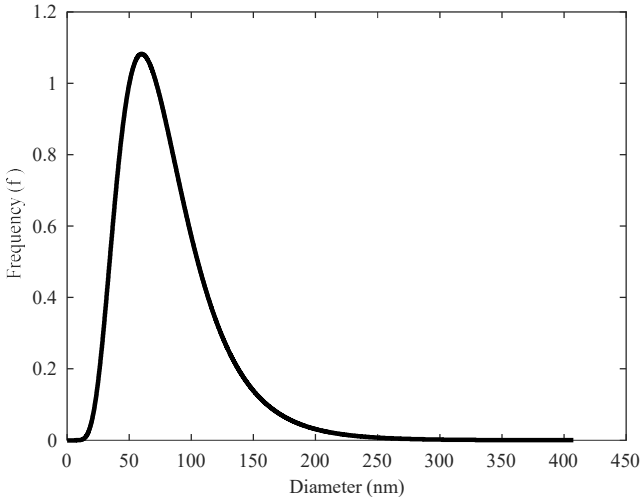

Figure 3: Case 2: Inlet droplet distribution

Based on this inlet distribution, the results are modelled in order to predict the outlet distribution as shown in Figure 4. The two diameters, giving the initial distribution in Figure 3 were respectively 81.5 and 100 nm, and were set as starting points for the simulation. It should be noted that several sets of diameters could be used and still been within the experimental data given with peak size about 60 nm and range being 10-440 nm. There is thus a degree of uncertainty in the initial diameters.

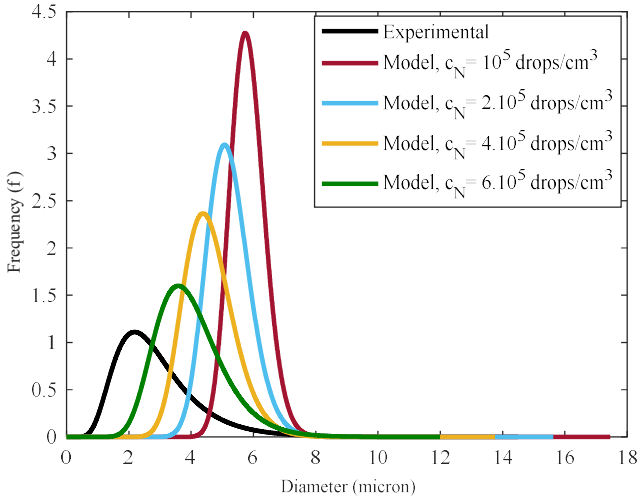

Figure 4: Case 2: Outlet droplet distribution

Toshiba measured the outlet droplet size distribution after the water wash and found that droplet sizes ranged from 0.5-7.3 μ in diameter while the peak size was around 2.2μ. Based on this, an outlet distribution was created and shown as the experimental distribution in Figure 4. As for the inlet distribution, the experimental outlet size distribution is uncertain. The modelled results for all number concentrations are also shown in Figure 4. It is seen that all modelled size distributions are in about the same range as the experimental one, although the peak sizes are higher than for the experimental distribution. The results of the modelling are deemed satisfactory taking into account that the droplets have grown from 81.5-100 nm to 1-8 μ. Also, no information is given in (Fujita, 2017) regarding possible use of a demister after the final water wash. Deposition of droplets inside the absorber, in the water wash section and in a demister will preferentially capture the larger droplets, thus reducing the peak size in the final droplet size distribution. These mechanisms are not included in the present model.

It can be seen that modelled distributions seem not to be able to catch the small droplets experimentally found in the outlet aerosol. In the model, all particles will grow and small particles actually grow faster than large ones. It is also a question how accurate the measurements of the small particles is.

From figure 4 it is seen that the size distributions and peak sizes move toward smaller sizes with increasing droplet number concentration. The reason is depletion of MEA in the gas phase at higher droplet number concentrations which reduces the growth rate.

There are other factors that may affect the results like choice of operational point in time, i.e. choice of number concentration and peak size from the experimental results provided in (Fujita, 2017). Also absorber and water wash characteristics are uncertain.

Thus, in order to test the model further, a later operating point in time was selected from (Fujita, 2017). The peak size was estimated to 85 nm and the inlet droplet size distribution estimated is presented in Figure 5. The two diameters, giving this initial distribution and peak size, were respectively 119.5 and 150 nm and were set as starting points for the simulation.

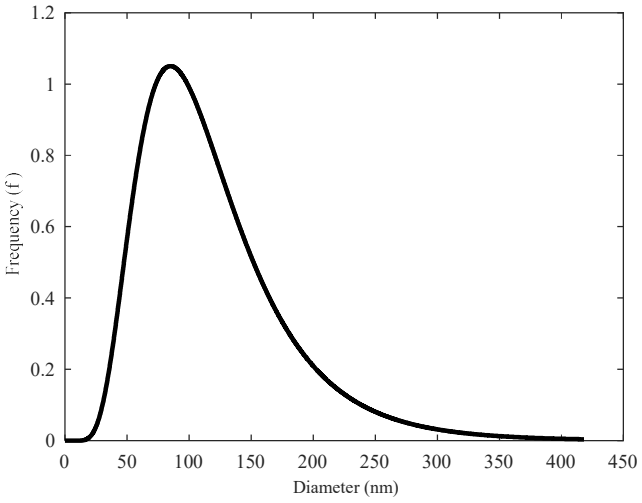

Figure 5: Case 2: Inlet droplet distribution

The predicted outlet droplet size distribution, together with experimental results, is presented in Figure 6. The experimental peak size and size range, (Fujita, 2017), were given as 2.6 μ and 0.5-7.5 μ respectively. The predicted size distributions in Figure 6 are seen, as for the previous case, to be higher than the experimental one, but to be relatively close. Also in this case possible deposition in absorber and demister may explain part of the deviations seen. Also, the experimental data are uncertain.

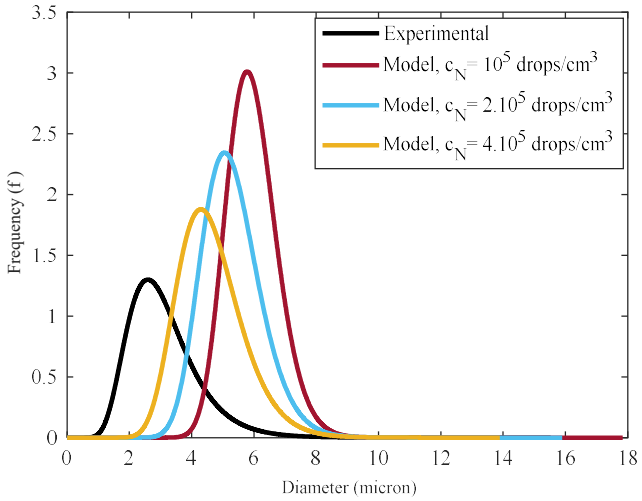

Figure 6: Case 2: Outlet droplet distribution

Case 3

(Majeed and Svendsen, 2018a) modelled the effect of different flue gas sources on composition and growth of mono-disperse aerosol droplet swarms. They also modelled different droplet number concentrations for each flue gas source and thus the amine take up in aerosol droplets for each case. The parameters and column profiles are given in (Majeed and Svendsen, 2018a), but further information is presented in table 2. The capture rate for CO_2 was 90% in all cases. In the current work the effect of flue gas source and droplet number concentration on the droplet size distribution will be discussed. Each flue gas source is modelled with droplet number concentrations, $c_N = 10^3$, 10^5 and 10^7 drops/cm^3 of gas.

Table 2: Column characteristics

Flue Gas, % CO2	Lean loading	Rich loading	Lean temp. (K)	Rich temp. (K)	L/G
4%	0.249	0.44	313.15	322.9	8.29
8%	0.249	0.5	313.15	322.11	2.69
12%	0.249	0.496	313.15	325.40	4.08
20%	0.249	0.49	313.15	332.38	7.0

Inlet droplet distribution:

A reasonable inlet droplet size distribution is generated by setting two initial sizes (diameters). Aerosol droplets of 0.3 μ and 0.34 μ were chosen to represent the inlet distribution in Eq. 12. The inlet distribution is presented in Figure 7.

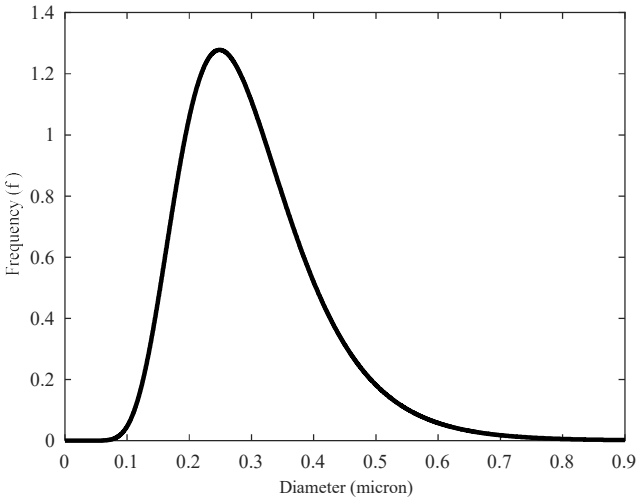

Figure 7: Case 3: Inlet droplet distribution

The inlet distribution shows that most of the droplets are in the range of 0.1 to 0.7 μ, which means that the distribution is not very widely dispersed. This is a result of the choice made in the inlet diameters being relatively close to each other. The distribution in Figure 7 is used as representing the inlet distribution for all flue gas sources and for all number concentrations.

After the inlet distribution is set, these initial conditions are used to model how the distribution changes through the absorber and in the water wash sections for case 3. Four different flue gas sources i.e. exhaust gas from natural gas, fuel oil and coal fired power plants and cement plants with respectively 4, 8, 12 and 20% CO_2 content were simulated in CO2SIM (Majeed and Svendsen, 2018) and the simulations used as basis for the droplet growth modelling. The droplet number concentrations considered were $c_N = 10^3$, 10^5 and 10^7 drops/cm^3 and results are presented in figures 8, 9, 10 and 11.

Outlet distributions:

Natural gas power plant:

In Figure 8 are shown the outlet droplet size distributions when natural gas is used as fossil fuel source. Figure 8a shows the outlet droplet size distribution for $c_N = 10^3$ drops/cm^3. While

Figures 8b and 8c represent outlet droplet distributions for c_N=10^5 and 10^7 drops/cm^3 respectively. We choose these droplet number concentrations based on experimental results from (Khakharia et al., 2013; Mertens et al., 2014) where it was found that most of the droplet number concentrations lie between c_N= 10^3 and 10^7 drops/cm^3. Thus, the concentrations chosen will cover the whole range of interest. The modelled results presented in (Majeed and Svendsen, 2018, 2017) show that composition, growth and amine uptake for c_N = 1 and 10^3 drops/cm^3 are, for all practical purposes, the same, so showing droplet distributions for c_N = 10^3 drops/cm^3 is enough. The droplet growth profiles are similar to Case 1, Figure 1 for two droplet model. For c_N = 10^3 drops/cm^3, the final peak droplet size after the water washes is around 3.8 µ. For this droplet concentration, the distribution width is somewhat reduced compared to the inlet distribution, and is also more symmetrical.

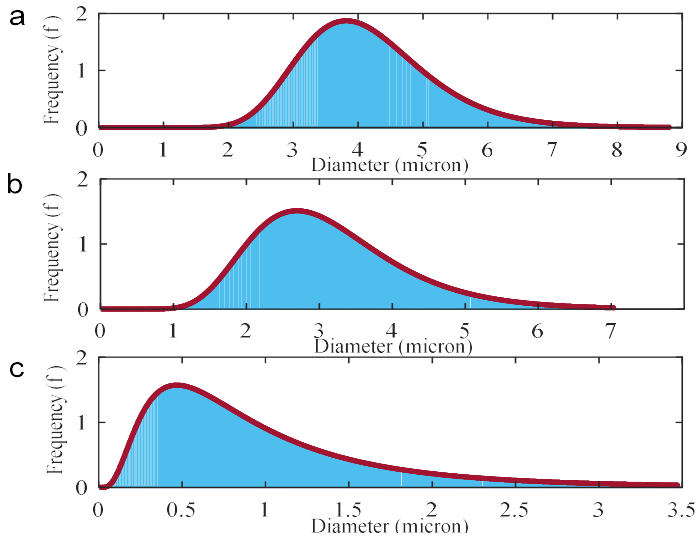

Figure 8: Case 3: Outlet distribution profiles for Natural Gas based flue gas (a) c_N= 10^3 drops/cm^3, (b) c_N= 10^5 drops/cm^3, (c) c_N= 10^7 drops/cm^3

As the droplet number concentration is increased, the final peak droplet diameter decreases. This is in line with experimental investigations (Fujita et al., 2017) as well as results presented in (Majeed and Svendsen, 2018, 2017). As the droplet number concentration increases, the MEA depletion of the gas phase becomes stronger and this will reduce the droplet growth. In case of c_N =10^5 drops/cm^3 the final droplet peak diameter is around 2.6-2.7 µ while with c_N = 10^7 drops/cm^3 the growth reduces significantly to a peak diameter of about 0.45 µ. From Figures 8 a-c, it is also seen that the final size distribution width increases with droplet number concentration. For c_N =10^5 drops/cm^3, shown in Figure 8b, the width is still reduced compared to the inlet distribution, but is wider than for c_N =10^3 drops/cm^3. Both the small change in peak size and distribution width when comparing Figures 8 a and b, indicates that gas phase MEA depletion is not so significant in case 8b. For c_N =10^7 drops/cm^3, shown in Figure 8c, both peak droplet diameter and width have changed considerably from the cases in Figures 8a and 8b. The final width is, in this case, about the same as for the inlet distribution and the peak size has only increased by a factor of 2.

Fuel Oil:

In Figure 9 a-c are shown the outlet size distributions for exhaust gas containing 8% CO_2.

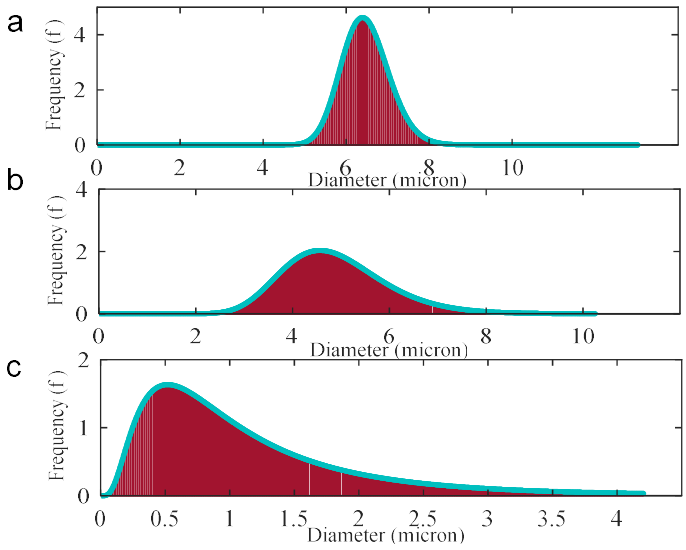

Figure 9: Case 3: Outlet distribution profiles for Fuel Oil based flue gas (a) $c_N = 10^3$ drops/cm^3, (b) $c_N = 10^5$ drops/cm^3, (c) $c_N = 10^7$ drops/cm^3

The results are qualitatively relatively similar to the natural gas exhaust gas case, see Figure 8. For $c_N = 10^3$ drops/cm^3, Figure 9a, we see that the peak diameter is about 6.4μ, which is an increase compared to Figure 8a. The width is reduced and the shape is as symmetrical as for Figure 8a. For $c_N = 10^5$ drops/cm^3, a reduction in peak diameter to about 4.5μ is seen. This reduction is, in relative terms, close to the same as seen in Figure 8. As for 4% CO_2 this indicates that the effect of number concentration is significant, but not very strong. For an increase in CO_2 content, the peak droplet sizes are seen to increase. This is in accordance with results in (Majeed and Svendsen, 2018). Also, for this droplet number concentration, the size distribution width is reduced compared to the 4% CO_2 case. For $c_N = 10^7$ drops/cm^3 the changes are stronger. The peak size is reduced to about 0.5μ, only slightly larger than for 4% CO_2, and the width is about same as shown in Figure 8c. It thus seems that the effect of CO_2 content is weaker at high droplet number concentrations, at least up to 8% CO_2 in the gas.

Coal:

In Figure 10 a-c are shown the outlet size distributions for exhaust gas containing 12% CO_2 based on the same inlet size distribution and the same droplet number concentrations as for previous cases. The predicted outlet droplet size distributions are qualitatively similar to the previous cases, but for the lower number concentrations, the distributions become narrower. For $c_N = 10^3$ drops/cm^3, seen in Figure 10a, the distribution is very narrow and the peak size has increased to more than 9μ. The reason for the narrower distributions at high CO_2 content is the stronger droplet growth. As seen earlier (Majeed and Svendsen, 2018) and Figure 1c, small droplets grow faster than large droplets. The two diameters characterizing the droplet distribution will thus close in on each other and this process will be stronger the more growth that takes place. As the amount of CO_2 in the flue gas increases, the droplets become larger, and thus the distribution narrows. For $c_N = 10^5$ drops/cm^3, also an increase in peak size is seen compared to the lower CO_2 concentrations. This increased growth results in a more narrow distribution, just as for the lower droplet number concentration. The results for $c_N = 10^5$

drops/cm^3 can be compared with the Case 2 results. The Exhaust gas CO_2 contents are about the same and the droplet number concentrations is within the range modelled in Case 2. The initial droplet sizes were smaller in Case 2, 81.5-100nm for Case 2 compared to 300-340nm in Case 3, and the distribution was narrower. The final peak size in Case 2 were 5.5-5.7µ, whereas in Case3 it is slightly higher than 6µ. This is reasonable as mentioned earlier, as smaller droplets grow faster than large ones.

For $c_N = 10^7$ drops/cm^3 a significant increase in peak droplet size is seen compared to the results for the lower CO_2 contents. It seems not to be any linear trend in the effect of CO_2 concentration on growth for the highest droplet number concentration. Also, the width of the distribution is significantly reduced compared to the lower CO_2 contents.

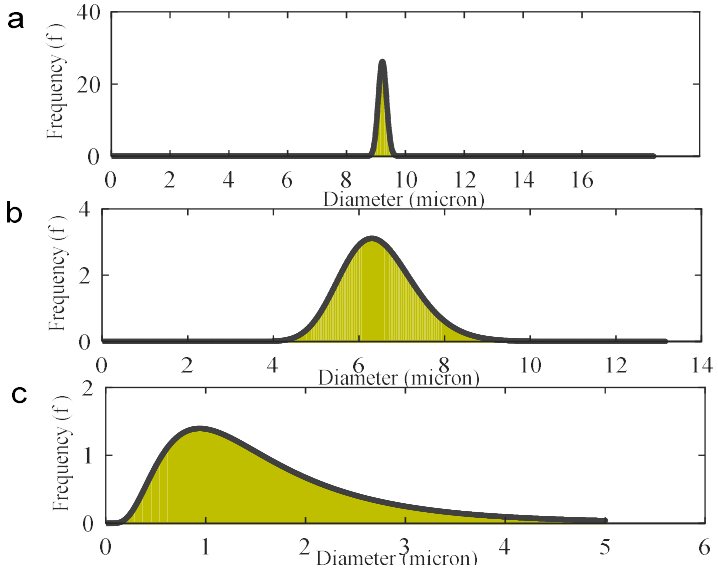

Figure 10: Case3: Outlet distribution profiles for Coal based flue gas (a) $c_N = 10^3$ drops/cm^3, (b) $c_N = 10^5$ drops/cm^3, (c) $c_N = 10^7$ drops/cm^3

Cement:

In Figure11 a-c are shown the outlet size distributions for exhaust gas containing 20% CO_2 based on the same inlet size distribution and the same droplet number concentrations as for previous cases. The same trends as seen for the lower CO_2 concentrations are seen in this case. For $c_N = 10^3$ drops/cm^3, the distribution is extremely narrow and the peak size has increased to nearly 13µ. Also for $c_N = 10^5$ drops/cm^3, the distribution is very narrow and the peak size has increased to about 8.5µ. A narrow size distribution and large peak size are advantageous for removing droplets in a demister with high efficiency. It was earlier found that high CO_2 contents gave higher emissions when the aerosol was untreated, see (Majeed and Svendsen, 2018) but with a demisting devise installed, the picture may be reversed. For $c_N = 10^7$ drops/cm^3, the peak droplet size has increased significantly compared to the lower CO_2 contents, to about

1.6µ. At the same time the distribution width has shrunk is now only about half of the inlet distribution. Droplet growth results are in agreement with (Majeed and Svendsen, 2018).

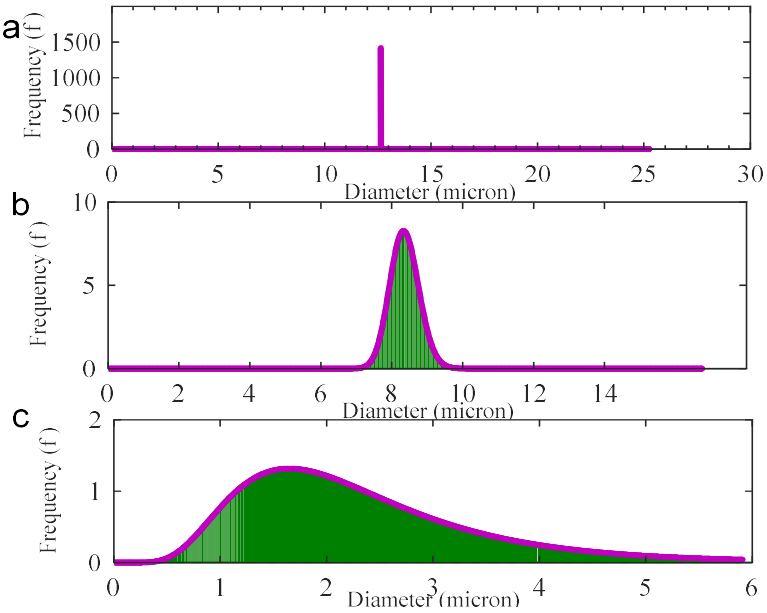

Figure 11: Case3: Outlet distribution profiles for Cement based flue gas (a) $c_N = 10^3$ drops/cm^3, (b) $c_N = 10^5$ drops/cm^3, (c) $c_N = 10^7$ drops/cm^3

Conclusions:

Identification of droplet size distributions is an important aspect when characterizing aerosol droplets in typical PCCC plant.
A multi droplet model is developed and validated in this work. Results are in agreement with single aerosol droplet model concerning specific cases (Majeed et al., 2017a; Majeed and Svendsen, 2017). A droplet size distribution model is developed based on the assumption of a log-normal size distribution. It is validated against pilot plant data from Toshiba (Fujita, 2017) and results are in reasonable agreement with the experimental data.

The effect of different flue gas sources is modelled using a given inlet distribution with droplets in the size range 0.1-0.7µ and with droplet number concentration varying from 10^3-10^7 drops/cm^3. Analyses of the predicted outlet size distributions show that as the amount of CO_2 in flue gas increases, droplet growth increases as well resulting in higher peak sizes. The main reasons for this are increased temperatures and higher CO_2 loading in the droplets at higher CO_2 concentrations. Also the outlet distributions become narrower with increasing CO_2 content. This is attributed to a more rapid size increase for small droplets compared to large ones, as also seen in earlier work.

The peak size decreases and the size distribution width increases with increasing droplet number concentration. This is caused by depletion of MEA from the gas phase resulting in slower droplet growth.

For a subsequent removal of droplets in a demister after the water wash section, a narrow size distribution and large size is advantageous. In this respect high CO_2 contents are better and

high droplet number concentrations, resulting in depletion of amine from the gas phase, is a disadvantage.

Acknowledgements:

Financial support from the Faculty of Natural Sciences at the Norwegian University of Science and Technology, Trondheim and the CLIMIT Demo project Aerosolve (616125) with partners SINTEF Materials and Chemistry, NTNU, Technology Center Mongstad, Maasvlakte CCS project (ROAD), Uniper, Energie Laborelec and TNO is greatly appreciated.

References:

Abu-Zahra, 2009. Carbon dioxide capture from flue gas: development and evaluation of existing and novel process concepts (PhD Thesis). Technical University of Delft, The Netherlands.

Ashgriz, N., 2011. Handbook of Atomization and Sprays: Theory and Applications. Springer Science & Business Media.

Biesenberger, J.A., Sebastian, D.H., 1983. Principles of polymerization engineering. Wiley.

da Silva, E.F., Kolderup, H., Goetheer, E., Hjarbo, K.W., Huizinga, A., Khakharia, P., Tuinman, I., Mejdell, T., Zahlsen, K., Vernstad, K., Hyldbakk, A., Holten, T., Kvamsdal, H.M., van Os, P., Einbu, A., 2013. Emission studies from a CO2 capture pilot plant. Energy Procedia 37, 778–783. https://doi.org/10.1016/j.egypro.2013.05.167

Davis, E.J., 1982. Transport Phenomena with Single Aerosol Particles. Aerosol Sci. Technol. 2, 121–144. https://doi.org/10.1080/02786828308958618

Dutcher, B., Fan, M., Russell, A.G., 2015. Amine-Based CO2 Capture Technology Development from the Beginning of 2013—A Review. ACS Appl. Mater. Interfaces 7, 2137–2148. https://doi.org/10.1021/am507465f

Fuchs, N. A., and Sutugin, A. 6. (1970). Highly Dispersed Aerosols, Ann Arbor Science Pub., Ann Arbor, MI.

Fujita, K., 2017. Effect of number concentration of aerosol in flue gas upstream of the absorber on mist based emissions from a PCC plant. 4th Post-Combustion Capture Conference (PCCC), Birmingham Alabama, Sept 2017..

Fujita, K., Muraoka, D., Kaseda, T., Saito, S., Kitamura, H., Kato, Y., Udatsu, M., Handa, Y., Suzuki, K., 2017. Impact of the Aerosol Particle Included in Actual Flue Gas on Amine Mist Formation/Growth in the Post-Combustion Capture Pilot Plant. Energy Procedia, 13th International Conference on Greenhouse Gas Control Technologies, GHGT-13, 14-18 November 2016, Lausanne, Switzerland 114, 930–938. https://doi.org/10.1016/j.egypro.2017.03.1235

Johnson, N.L., Kotz, S., Balakrishnan, N., 1994. Continuous Univariate Distributions, Vol. 1, 2 edition. ed. Wiley-Interscience, New York.

Kamijo, T., Kajiya, Y., Endo, T., Nagayasu, H., Tanaka, H., Hirata, T., Yonekawa, T., Tsujiuchi, T., 2013. SO3 Impact on Amine Emission and Emission Reduction Technology. Energy Procedia, GHGT-11 Proceedings of the 11th International Conference on Greenhouse Gas Control Technologies, 18-22 November 2012, Kyoto, Japan 37, 1793–1796. https://doi.org/10.1016/j.egypro.2013.06.056

Khakharia, P., Brachert, L., Mertens, J., Huizinga, A., Schallert, B., Schaber, K., Vlugt, T.J.H., Goetheer, E., 2013. Investigation of aerosol based emission of MEA due to sulphuric acid aerosol and soot in a Post Combustion CO2 Capture process. Int. J. Greenh. Gas Control 19, 138–144. https://doi.org/10.1016/j.ijggc.2013.08.014

Koch, G., 2015. Koch-Glitsch | Mass transfer and mist elimination equipment design and manufacture [WWW Document]. URL http://www.koch-glitsch.com/default.aspx (accessed 9.9.17).

Luo, H., Svendsen, H.F., 1996. Theoretical model for drop and bubble breakup in turbulent dispersions. AIChE J. 42, 1225–1233. https://doi.org/10.1002/aic.690420505

Majeed, H., Knuutila, H., Hillestad, M., Svendsen, H.F., 2017a. Gas phase amine depletion created by aerosol formation and growth. Int. J. Greenh. Gas Control 64, 212–222. https://doi.org/10.1016/j.ijggc.2017.07.001

Majeed, H., Knuutila, H.K., Hillestad, M., Svendsen, H.F., 2017b. Characterization and modelling of aerosol droplet in absorption columns. Int. J. Greenh. Gas Control 58, 114–126. https://doi.org/10.1016/j.ijggc.2017.01.006

Majeed, H., Svendsen, H.F., 2018a. Characterization of Aerosol Emissions from CO2 Capture Plants treating various Power Plant and Industrial Flue Gases. Int. J. Greenh. Gas Control 74, 282–295. https://doi.org/10.1016/j.ijggc.2018.04.016

Majeed, H., Svendsen, H.F., 2018b. Effect of Water Wash on Mist and Aerosol Formation in Absorption Column. Chem. Eng. J., 333(2018),636-648, https://doi.org/10.1016/j.cej.2017.09.124

Marchetti, J.M., Svendsen, H.F., 2012. Review of Kernels for Droplet-Droplet Interaction, Droplet-Wall Collision, Entrainment, Re-Entrainment, and Breakage. Chem. Eng. Commun. 199, 551–575. https://doi.org/10.1080/00986445.2011.592453

Mertens, J., Brachert, L., Desagher, D., Thielens, M.L., Khakharia, P., Goetheer, E., Schaber, K., 2014. ELPI+ measurements of aerosol growth in an amine absorption column. Int. J. Greenh. Gas Control 23, 44–50. https://doi.org/10.1016/j.ijggc.2014.02.002

Moser, P., Schmidt, S., Stahl, K., Vorberg, G., Lozano, G.A., Stoffregen, T., Richter, T., 2015. The wet electrostatic precipitator as a cause of mist formation—Results from the amine-based post-combustion capture pilot plant at Niederaussem. Int. J. Greenh. Gas Control 41, 229–238. https://doi.org/10.1016/j.ijggc.2015.07.010

Rochelle, G.T., 2009. Amine Scrubbing for CO2 Capture. Science 325, 1652–1654. https://doi.org/10.1126/science.1176731

Schaber, K., 1995. Aerosol formation in absorption processes. Chem. Eng. Sci. 50, 1347–1360. https://doi.org/10.1016/0009-2509(95)98846-7